ROBOMECH Journal

RESEARCH

Open Access

Length control of a McKibben pneumatic actuator using a dynamic quantizer

Yasuhiro Sugimoto[1*], Keisuke Naniwa[1†], Daisuke Nakanishi[2†] and Koichi Osuka[1†]

Abstract

McKibben pneumatic actuators (MPAs) are soft actuators that exert tension by applying compressed air to expand a rubber tube. Although electro-pneumatic regulators can control air pressure, most are large and expensive. This study utilizes a dynamic quantizer to control the MPA with a small solenoid valve that can only open and close the valve instead of an electro-pneumatic regulator. A dynamic quantizer is one of the quantizers that converts continuous signals to discrete signals. Our previous study confirmed that tension control of MPA under isometric conditions could be realized using a dynamic quantizer. However, it is often necessary to control the length of the MPA as well as the tension of the MPA. This study implements a dynamic quantizer to control the length of the MPA with a small solenoid valve. Numerical simulations and experimental tests verify the effectiveness of the proposed method. The results of the numerical simulations and experimental tests confirmed that the length of the MPA can be controlled using the dynamic quantizer.

Keywords McKibben pneumatic actuator, Dynamic quantizer, Length control

Introduction

The McKibben pneumatic actuator (MPA) is a soft actuator developed by J.L. McKibben in 1961, primarily to assist patients with severe flaccid paralysis of the upper limb. In the same year, mimicking the grasping and releasing motions of a patient's hand was achieved by attaching an assistive device using an MPA [1]. Subsequently, several non-medical studies have been conducted, such as developing a robotic arm with an antagonistically placed MPA [2]. Since then, its applications have extended beyond the medical field, with studies exploring their use in robotic arms owing to their flexibility, lightweight properties, and high power output, and have achieved dynamic robot motions [3–7].

Enhancing the control capabilities of these actuators is crucial to improving the performance of MPA-driven robots. Several studies have been conducted to control the exerted tension or length of the pneumatic actuators [8–12]. In the control of MPAs, proportional pneumatic valves, including electro-pneumatic regulators have been used to control the pressure applied to pneumatic actuators. Although electro-pneumatic regulators can accurately control the pressure, they are large and expensive. Alternatively, compact solenoid valves that offer discrete on-off control have emerged as viable pneumatic control devices. Integrating these small solenoid valves into MPA control systems can considerably advance the development of robots using multiple actuators.

It is necessary to convert continuous pressure inputs into discrete on-off values to achieve MPA control using small solenoid valves. Prior studies proposed control methods such as sliding mode control [13] or modified pulse-width modulation (PWM) techniques [14, 15]. However, these control methods require precise models

†Keisuke Naniwa, Daisuke Nakanishi and Koichi Osuka have contributed equally to this work.

*Correspondence:
Yasuhiro Sugimoto
yas@mech.eng.osaka-u.ac.jp
[1] Department of Mechanical Engineering, Osaka University, 2-1, Yamadaoka, Suita, Osaka 565-0871, Japan
[2] Department of Control Engineering, National Institute of Technology, Matsue College, 14-4, Nishiikuma, Matsue, Shimane 690-8518, Japan

or tuning of multiple thresholds, such as flow dynamics based on valve opening and closing or tuning multiple thresholds at which the valve opens or closes relative to the command value. In this study, we focus on dynamic quantizers that convert continuous-valued signals into discrete-valued signals without relying on detailed models or the response characteristics of quantization devices [16, 17]. Moreover, dynamic quantizers can easily be integrated into feedback control systems designed for continuous-valued inputs. Thus, a straightforward replacement for electro-pneumatic regulators using small solenoid valves can be achieved.

In our previous research [18], we proposed a control method for MPA tension that utilizes dynamic quantizers to convert continuous pressure inputs into discrete on-off values, enabling control of small solenoid valves with binary operation capabilities. In addition, we experimentally verified the effectiveness of this control method using actual equipment. However, the study primarily focused on controlling the tension of MPAs under isometric conditions. The MPA length changes when used as an actuator for a robot, such as when driving a joint. Therefore, relaxing the isometric condition is crucial to leverage fully the control capabilities of MPAs using dynamic quantizers.

Therefore, this study employed a control method utilizing dynamic quantizers and solenoid valves with binary operation capabilities to a nonisometric MPA model for length control. Simulations and experiments demonstrated that this control method effectively regulates MPA's length. The results of this study indicate that the proposed control method can be adapted to diverse scenarios to realize more varied motions in robots using MPAs.

Model of MPA-mass system

McKibben pneumatic actuator (MPA)

Figure 1 shows the MPA comprising rubber tube, mesh sleeve, and intake and exhaust terminals used in this study. The MPA is driven by applying air pressure to the rubber tube. The sleeve fibers prevent the rubber tube from expanding in the radial direction. Therefore, the internal pressure in the rubber tube acts in the axial direction only, yielding contraction and tension in that direction. This mechanism and using air as the working fluid allow the MPA to achieve lightweight and high-powered motion. Additionally, its physical flexibility allows higher elasticity and back-drivability than that of other actuators such as motors. Because of these characteristics, MPA helps an actuator to achieve dynamic motions in robotic applications.

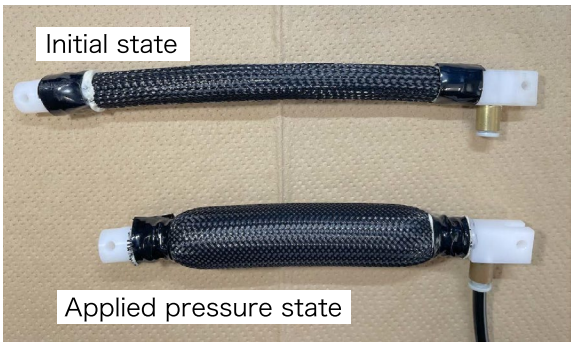

Fig. 1 Overview of McKibben pneumatic actuator: MPA (top) before and (bottom) after air pressure application (0.4 MPa)

Various tension models have been developed for MPAs [19–24]. This study used the linear approximation model proposed in our previous study as the tension model for MPA [24]. It has been confirmed that this model can appropriately express the tension characteristics of MPA despite its simplistic form, as compared to other proposed models.

In the linear approximation model, the exerted tension $f_m(t)$ is defined as

$$f_m(t) = S_1P(t) + S_2P(t)L(t) + S_3L(t) + S_4 - \gamma\dot{L}(t) \tag{1}$$

where S_1, S_2, S_3, S_4, and γ are the constant coefficients determined from the material properties of the MPA. Thus, the exerted tension of the MPA is determined by the length of the MPA ($L(t)$), contraction velocity ($\dot{L}(t)$), and applied pressure ($P(t)$).

MPA-mass system

The system to be controlled has a simple configuration, as shown in Fig. 2. We verify the feasibility of MPA length control by connecting a weight to the MPA via a wire, while connecting the other end to a fixed end. We control the position of the weight by controlling the length (amount of contraction) of the MPA.

Let m be the mass of the weight, g be the acceleration due to gravity, and $x(t)$ be the contraction length of MPA from its unloaded length L_0; that is, $L(t) = L_0 - x(t)$. The mass of MPA was assumed to be sufficiently small compared with the mass of the weight.

The equation of motion for $x(t)$ becomes

$$\begin{aligned} m\ddot{x}(t) &= f_m(t) - mg \\ &= S_1P(t) + S_2P(t)(L_0 - x(t)) + S_3(L_0 - x(t)) + S_4 - \gamma\dot{x}(t) - mg \\ &= -S_3x(t) - \gamma\dot{x}(t) - S_2P(t)x(t) + (S_1 + S_2L_0)P(t) + S_3L_0 + S_4 - mg \end{aligned} \tag{2}$$

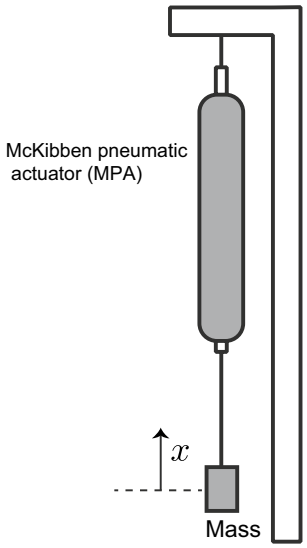

Fig. 2 The MPA-mass system

Assuming that the variation in $x(t)$ is sufficiently small compared to that of $P(t)$, we approximate $P(t)x(t) \approx P(t)\bar{x}$ where $\bar{x}$ is a constant. Using this approximation, Eq. (2) can be rewritten as

$$\begin{aligned} m\ddot{x}(t) &= -S_3x(t) - \gamma\dot{x}(t) + (S_1 + S_2L_0 - S_2\bar{x})P(t) + S_3L_0 + S_4 - mg \\ &= -S_3x(t) - \gamma\dot{x}(t) + \alpha P(t) + \beta \end{aligned} \tag{3}$$

where $\alpha = S_1 + S_2L_0 - S_2\bar{x}$, $\beta = S_3L_0 + S_4 - mg$.

Using $X(t) = x(t) - \frac{\beta}{S_3}$, Eq. (3) can be rewritten as

$$\ddot{X}(t) = -\frac{S_3}{m}X(t) - \frac{\gamma}{m}\dot{X}(t) + \frac{\alpha}{m}P(t) \tag{4}$$

Equation (4) can be further rewritten as the following state-space representation:

$$\begin{cases} \begin{bmatrix} \dot{X}(t) \\ \ddot{X}(t) \end{bmatrix} = \begin{bmatrix} 0 & 1 \\ -\frac{S_3}{m} & -\frac{\gamma}{m} \end{bmatrix} \begin{bmatrix} X(t) \\ \dot{X}(t) \end{bmatrix} + \begin{bmatrix} 0 \\ \frac{\alpha}{m} \end{bmatrix} P \\ y(t) = \begin{bmatrix} 1 & 0 \end{bmatrix} \begin{bmatrix} X(t) \\ \dot{X}(t) \end{bmatrix} \end{cases} \tag{5}$$

The delay in the air supply to the MPA is expressed as a first-order lag system, as follows:

$$\begin{cases} \tau\dot{x}_p(t) + x_p(t) = P(t) \\ \tilde{P}(t) = x_p(t) \end{cases} \Rightarrow \begin{cases} \dot{x}_p(t) = -\frac{1}{\tau}x_p(t) + \frac{1}{\tau}P(t) \\ \tilde{P}(t) = x_p(t) \end{cases} \tag{6}$$

where $x_p(t)$ is the state, τ is the time constant, and $\tilde{P}(t)$ is the delayed system output.

Since the input to system (5) is the output of the delay system $\tilde{P}(t)$, the system to be controlled can be derived using Eqs. (5) and (6), as follows:

$$\begin{cases} \begin{bmatrix} \dot{x}_p(t) \\ \dot{X}(t) \\ \ddot{X}(t) \end{bmatrix} = \begin{bmatrix} -\frac{1}{\tau} & 0 & 0 \\ 0 & 0 & 1 \\ \frac{\alpha}{m} & \frac{-S_3}{m} & -\frac{\gamma}{m} \end{bmatrix} \begin{bmatrix} x_p(t) \\ X(t) \\ \dot{X}(t) \end{bmatrix} + \begin{bmatrix} \frac{1}{\tau} \\ 0 \\ 0 \end{bmatrix} P(t) \\ y(t) = \begin{bmatrix} 0 & 1 & 0 \end{bmatrix} \begin{bmatrix} x_p(t) \\ X(t) \\ \dot{X}(t) \end{bmatrix} \end{cases} \tag{7}$$

In the following sections, we explain the design of the controllers and dynamic quantizers based on this system.

Dynamic quantizer

Instead of inputting the continuous value u directly to plant P, a discretized input v was used (Fig. 3). A quantizer Q can convert u to v to control the MPA length with a solenoid valve that can be opened and closed.

In this study, a dynamic quantizer was used as the quantization method [16]. The dynamic quantizer makes the input–output characteristics of the system with quantizer close to that of an ideal system without a quantizer.

In a previous study, various types of quantized systems were considered. Figure 4 shows the feedback system with an input quantizer.

P denotes a discrete-time linear plant.

$$P : \begin{cases} x(k+1) = Ax(k) + Bv(k) \\ z(k) = C_1x(k) \\ y(k) = C_2x(k) \end{cases} \tag{8}$$

where $x(k) \in \mathbf{R}^{n_p}$ is the state, $v(k) \in \mathbf{R}^m$ are the inputs, $z(k) \in \mathbf{R}^{l_1}$ and $y(k) \in \mathbf{R}^{l_2}$ are the outputs. $A \in \mathbf{R}^{n_p \times n_p}$, $B \in \mathbf{R}^{n_p \times m}$, $C_1 \in \mathbf{R}^{l_1 \times n_p}$, and $C_2 \in \mathbf{R}^{l_2 \times n_p}$ are constant matrices. n_p, l_1, l_2, and m denote the dimensions of $x(k)$, $z(k)$, $y(k)$, and $v(k)$ respectively.

K is a discrete-time controller.

$$K : \begin{cases} x_K(k+1) = A_Kx_K(k) + B_{K1}r(k) + B_{K2}y(k) \\ u(k) = C_Kx_K(k) + D_{K1}r(k) + D_{K2}y(k) \end{cases} \tag{9}$$

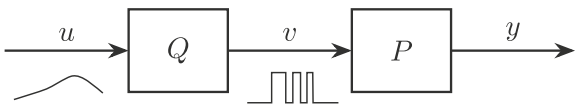

Fig. 3 Quantizer that converts continuous value input in the plant to discrete value input

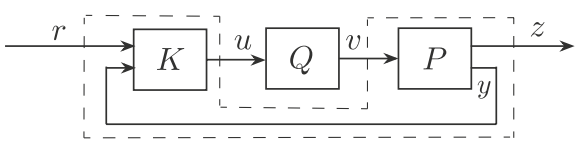

Fig. 4 Feedback system with input quantizer

where $x_K(k) \in \mathbf{R}^{n_k}$ is the state, $r(k) \in \mathbf{R}^r$ is the reference input, and $A_K \in \mathbf{R}^{n_k \times n_k}$, $B_{K1} \in \mathbf{R}^{n_k \times r}$, $B_{K2} \in \mathbf{R}^{n_k \times l_2}$, $C_K \in \mathbf{R}^{m \times n_k}$, $D_{K1} \in \mathbf{R}^{m \times r}$, and $D_{K2} \in \mathbf{R}^{m \times l_2}$ are constant matrices. n_k and r are the dimensions of $x_K(k)$ and $r(k)$, respectively.

The dynamic quantizer Q is given by

$$Q : \begin{cases} \xi(k+1) = A_Q \xi(k) + B_{Q1} u(k) + B_{Q2} v(k) \\ v(k) = q(C_Q \xi(k) + u(k)) \end{cases} \tag{10}$$

where $\xi(k) \in \mathbf{R}^N$, $v(k) \in \mathbf{V}^m := \{0, \pm d, \pm 2d, \cdots\}^m$, and $u(k) \in \mathbf{R}^m$ denote the state, output, and input of the quantizer, respectively. $A_Q \in \mathbf{R}^{N \times N}$, $B_{Q1}, B_{Q2} \in \mathbf{R}^{N \times m}$, and $C_Q \in \mathbf{R}^{m \times N}$ are constant matrices. N denotes the number of dimensions of $\xi(k)$. $\mathbf{V}$ is a discrete set specified by the quantization interval $d \in \mathbf{R}_+$. The function q: $\mathbf{R}^m \to \mathbf{V}^m$ is the nearest-neighbor static quantizer approaching $-\infty$. An example of the case $m := 1$ is shown in Fig. 5. The static quantizer shown in this figure is also a quantizer. Similarly, PWM, used for motor control, is also a quantizer. Equation (10) shows that the dynamic quantizer is a dynamical system with a state. Therefore, dynamic quantizers are expected to perform better than PWMs if A_Q, B_{Q1}, B_{Q2}, and C_Q are appropriately selected.

Let T denote the performance evaluation time for Q. $Z_Q(x_0, R)$ is defined by the sequence of output z for input $R := (r_0, r_1, \cdots, r_{T-1})$ and the initial value x_0. For an unquantized system Σ_I using continuous-value inputs without a dynamic quantizer, the symbol $Z_I(x_0, R)$ is defined similarly. The dynamic quantizer design problem for the target discrete-time system (8) and the controller (9) is defined as finding A_Q, B_{Q1}, B_{Q2}, and C_Q in Eq. (10), which minimizes the following performance index of the quantizer:

$$E(Q) := \sup_{x_0, R} ||Z_Q(x_0, R) - Z_I(x_0, R)||.$$

Under certain conditions, a solution to the design problem can be analytically derived [16, 25]. Otherwise, computer-based numerical optimization methods are used to identify dynamic quantizers [26, 27]. Implementing these methods based on prior research can be challenging. However, some quantizer design tools are available, such as the MATLAB toolbox (ODQ toolbox [28], ODQ Lab [29]), and the Python library (NQLib) [30], are available to solve the design problem through numerical optimization using a linear programming problem. These tools provide A_Q, B_{Q1}, B_{Q2}, and C_Q using only Eqs. (8) and (9), facilitating the implementation of dynamic quantizers in real systems.

Therefore, this study proposes using a dynamic quantizer as a new method to control the MPA length with a solenoid valve that can only be opened and closed. The dynamic quantizer converts the continuous pressure input into a binary input. The solenoid valve is driven based on the dynamic quantizer output. Specifically, a controller was designed for system (7), and a dynamic quantizer was designed for the system and controller.

In the following sections, we verified the feasibility of controlling the length of MPA using the designed dynamic quantizer and a solenoid valve through simulations and experiments.

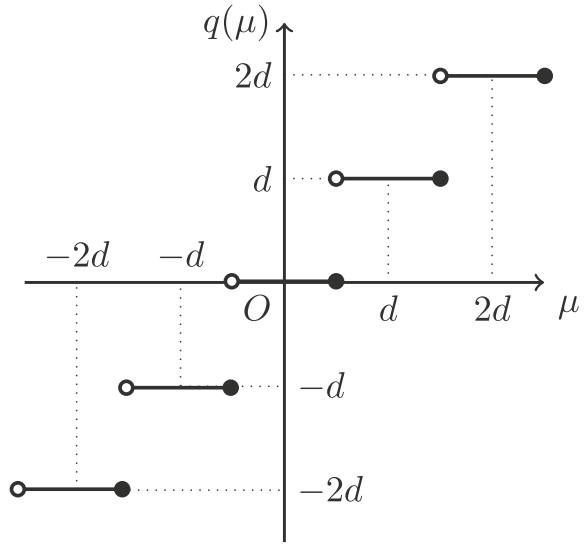

Fig. 5 Static quantizer $q(\mu)$ for $\mu \in \mathbf{R}^1$

Numerical simulation

First, the effectiveness of MPA length control using dynamic quantizers was verified through numerical simulations.

Design of controller

Discretizing Eq. (7) using a zero-order hold and $T_s = 0.01$ s, the following discrete-time system can be derived:

$$\begin{cases} \dot{x}_d(k+1) = \begin{bmatrix} 0.98758 & 0 & 0 \\ 0.0060683 & 0.97109 & 0.0064680 \\ 1.0450 & -4.9918 & 0.37905 \end{bmatrix} x_d(k) \\ \qquad\qquad + \begin{bmatrix} 0.012422 \\ 0.000027188 \\ 0.0075854 \end{bmatrix} P(k) \\ y(k) = \begin{bmatrix} 0 & 1 & 0 \end{bmatrix} x_d(k) \end{cases} \tag{11}$$

where k is the discretized time and $x_d(k)$ is the state of k. We derived the constant coefficients in Eq. (1) based on a previous study [24] as $S_1 = -3358.9$, $S_2 = 16884.0$, $S_3 = 1686.3$, $S_4 = -516.46$, and $\gamma = 200$. We used $L_0 = 0.290$ m, $\bar{x} = 0.07$ m, $m = 2.185$ kg. These values

were determined using the experimental system for validation. The time constant τ of the delay in Eq. (6) was derived experimentally from the step response. A step input of 0.4 MPa was applied to the actual MPA via a solenoid valve. From the time required for the step response to reach 63.2% of the steady state, we derive τ as 0.800 s.

In this study, the following discrete-time PI controller was used to control contraction x of the MPA:

$$\begin{aligned} x_K(k+1) &= x_K(k) + 0.01y(k) \\ u(t) &= 10.0x_K(k) + 10.0y(k) \end{aligned} \tag{12}$$

where $x_K(k)$ denotes the controller state. The PI controller was selected to provide sufficient tracking performance when controlling the contraction x without a dynamic quantizer.

For systems (11) and (12), the dynamic quantizer is designed using NQLib [30]. The obtained 1-dimension dynamic quantizers were $A_Q = 0.20000$, $B_Q = 0.44721$, and $C_Q = -0.44721$. The performance index $E(Q)$ was 0.0015528 m. Here, the quantization interval of the static quantizer $q(z)$ was set to $d = 0.4$ MPa, indicating that the pressure input value was quantized to a discrete value in 0.4 MPa increments.

Simulation result

Using the derived dynamic quantizer, numerical simulations were performed to verify whether the MPA contraction can be controlled by turning the valve on or off. The control target in the simulation was not a discretized linear model (11), but a nonlinear model (2). The dynamic quantizer quantized the input in increments of $d = 0.4$ MPa using the dynamic quantizer. Therefore, there are cases in which the quantized input has values other than 0 and 0.4 MPa. With the given solenoid valve, the input to the system was 0.4 and 0 MPa if the quantized input was above 0.4 MPa and below 0 MPa, respectively.

As the target trajectory $\tilde{x}$ of the contraction length of MPA x, we use

- Step reference $\tilde{x}(k) = 0.01, 0.02, 0.03, 0.04, 0.05$ m,
- Sinusoidal reference $\tilde{x}(k) = 0.02(1 - \cos(2\pi f T_s k))$ m where $f = 0.1, 0.2$,
- Staircase reference $\tilde{x}(k) = 0.02, 0.03, 0.04$ m.

Simulation results for each target trajectory are shown in Figs. 6 ~ 13. The upper, middle, and lower parts represent the contraction x, the pressure input, and the enlarged pressure input, respectively. In the figure investigating contraction length x, the red and blue lines indicate results with and without the dynamic quantizer; the dotted line represents target trajectories. The result without a dynamic quantizer is the result when the continuous value calculated by the PI controller was used as input to MPA without passing through the dynamic quantizer. In the pressure input figure, the green and red lines represent continuous input before quantization and the results with the dynamic quantizer, respectively. The enlarged graph of pressure input shows the pressure input from the beginning of the simulation to a few seconds after to clarify how the valve is switched on and off. From simulation results, rising time, 5% settling time, and RMSE of the last 3 s for step references were calculated. The average phase delay from the target trajectory for the sinusoidal references was also calculated. These results are shown in Tables 1 and 2, respectively.

Although a slight oscillation remains for the target trajectory, x follows without a steady deviation, almost the same as in the case without a dynamic quantizer. The proposed method using the dynamic quantizer uses discrete value inputs of only 0 and 0.4 MPa, while the method without the dynamic quantizer uses continuous value inputs. Therefore, the proposed method

Table 2 Comparison of control performance with and without dynamic quantizer for sinusoidal target references

Frequency f (Hz)	Phase delay (rad)	
	With	Without
0.1	0.05184	0.3305
0.2	0.4800	0.5234

Table 1 Comparison of control performance with and without dynamic quantizer for step target references

Reference (m)	Rising time (sec)		Settling time (sec)		RMSE (m)	
	With	Without	With	Without	With	Without
0.01	2.369	0.095	9.971	1.003	3.447×10^{-4}	5.342×10^{-7}
0.02	1.836	0.151	2.927	0.365	3.151×10^{-4}	8.792×10^{-7}
0.03	1.322	0.217	2.201	0.480	6.872×10^{-5}	1.558×10^{-6}
0.04	0.719	0.359	1.476	0.892	9.401×10^{-5}	3.288×10^{-6}
0.05	0.424	0.597	0.959	1.283	6.829×10^{-5}	1.007×10^{-5}

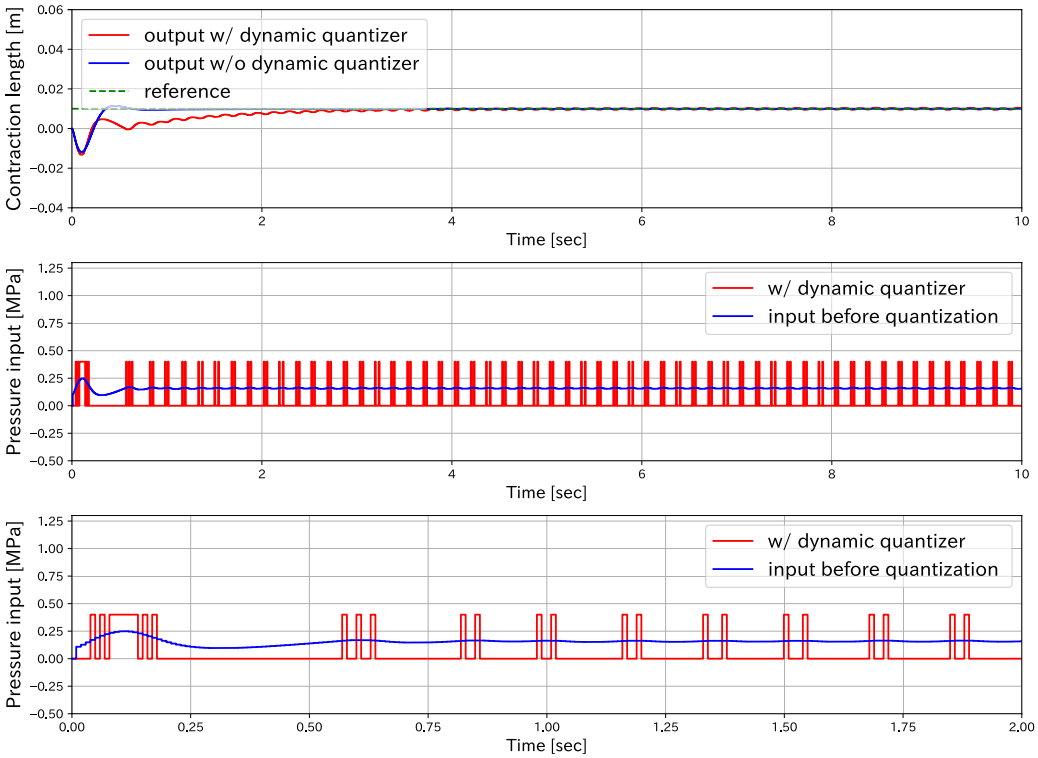

Fig. 6 Simulation result for a step reference $\bar{x}(k) = 0.01$ m

using the dynamic quantizer is estimated to have worse control performance than the control method without the dynamic quantizer basically. From Figs. 6, 7, 8, 9 10 and Table 1, it can be confirmed that the control performance was degraded, but the degree of degradation was not significant. On the contrary, for the step reference of $\bar{x}(k) = 0.05$ m, the rise time and settling time are better with the proposed method. Figure 11 shows that the response at the time of target reference changeover is slightly better than that obtained using the dynamic quantizer. Figures 12, 13 and Table 2 show a slight delay in following the sinusoidal target trajectory without a dynamic quantizer. This is attributed to the delay in the application of air pressure. However, with the dynamic quantizer, the delay is reduced. Therefore, it can be confirmed that, depending on the conditions, the control performance can be improved using the dynamic quantizer. This increased control performance or responsiveness may be because the quantization applies a pressure input that is instantaneous but larger than the value calculated by the PI controller. It has been reported that a feedback modulator, as one of the quantizers, can compensate for nonlinear factors, such as response delay, deadband elements, and backlash [31, 32]. Dynamic quantizers may have similar properties, but the analysis of this effect is a subject for future work.

From the pressure input figures, it can be confirmed that the continuous-value input was converted into a discrete-value input of $d = 0.4$ MPa for any target value. In all cases, the continuous value of the pressure input under the steady state ranged from 0 to 0.4 MPa. This pressure input was challenging to achieve using solenoid valves, which can be opened or closed state and only use either 0 or 0.4 MPa as the input pressure. A dynamic quantizer helps realize the required pressure input and achieve tracking control. These results confirm the effectiveness of the proposed method using a dynamic quantizer for MPA length control.

In all the simulations, the transient response exhibits oscillations probably because the MPA tension model (1) does not fully reflect the elongation behavior from the natural length. In actual equipment, MPAs rarely extend beyond their unloaded length and contract to a large extent. Therefore, with MPA, the system is expected to converge without large oscillations in the transient response and track the target reference.

Experimental verification

Experiments were conducted to verify the feasibility of controlling length tracking using the dynamic quantizer.

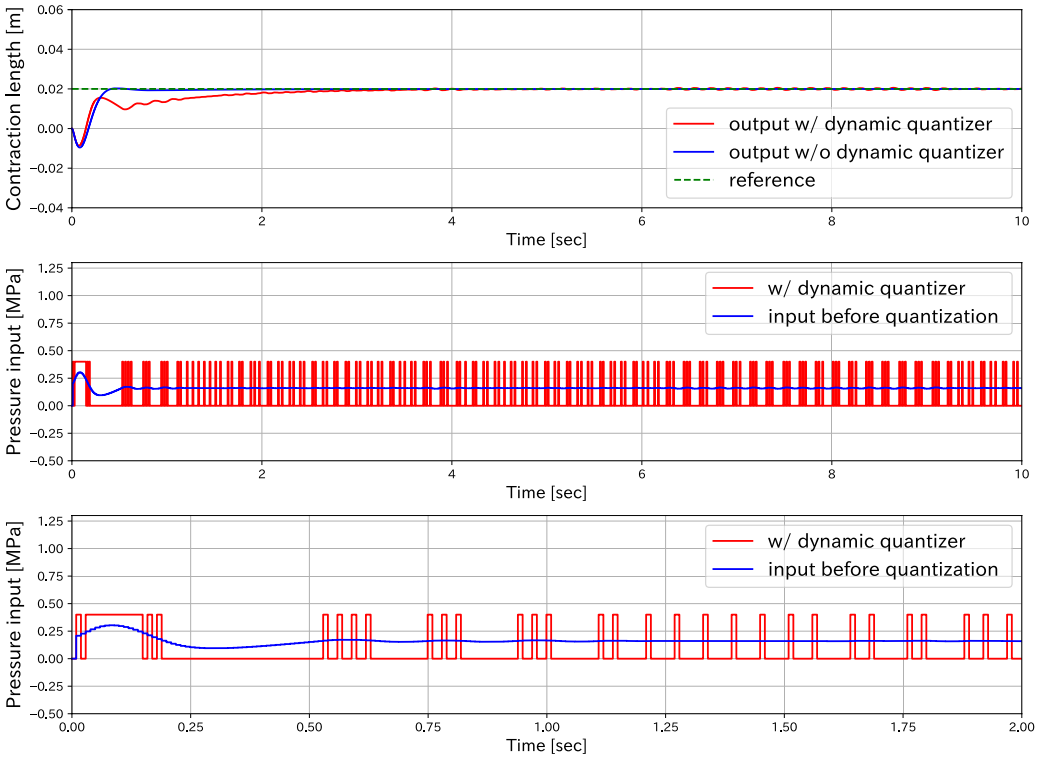

Fig. 7 Simulation result for a step reference $\bar{x}(k) = 0.02$ m

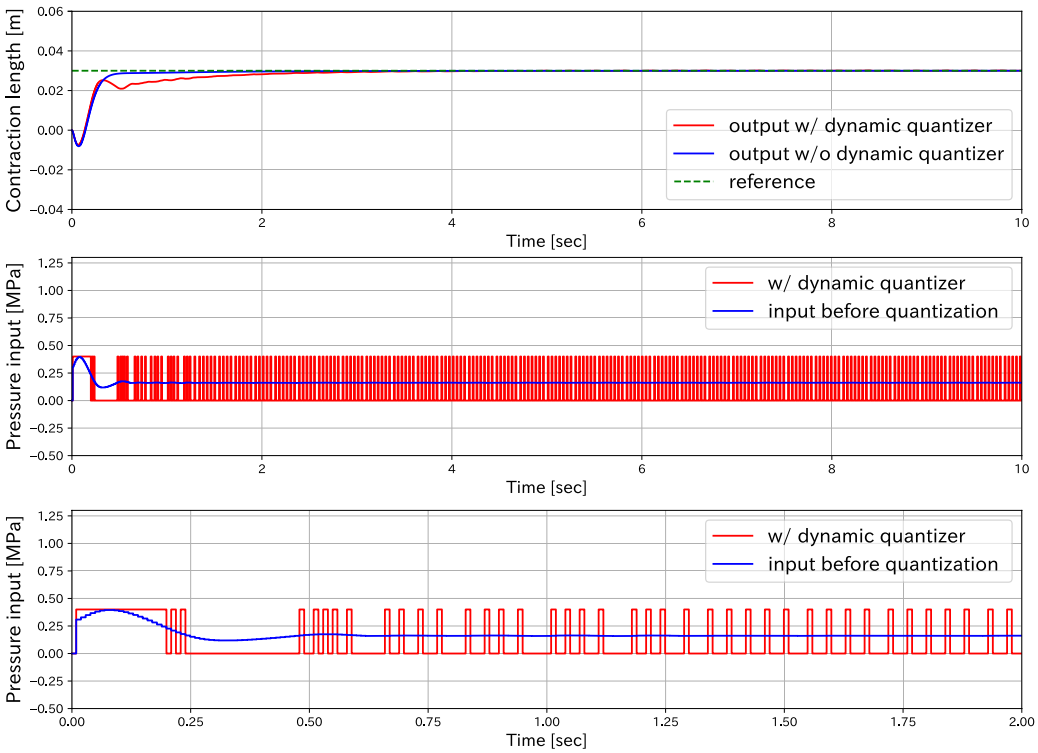

Fig. 8 Simulation result for a step reference $\bar{x}(k) = 0.03$ m

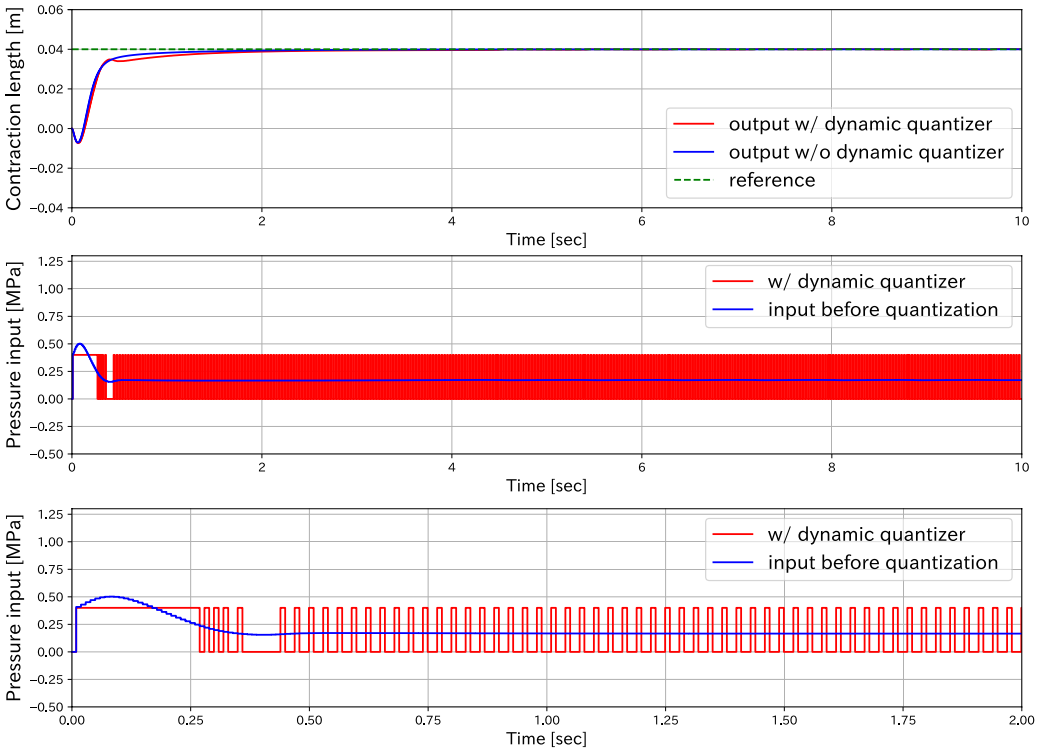

Fig. 9 Simulation result for a step reference $\bar{x}(k) = 0.04$ m

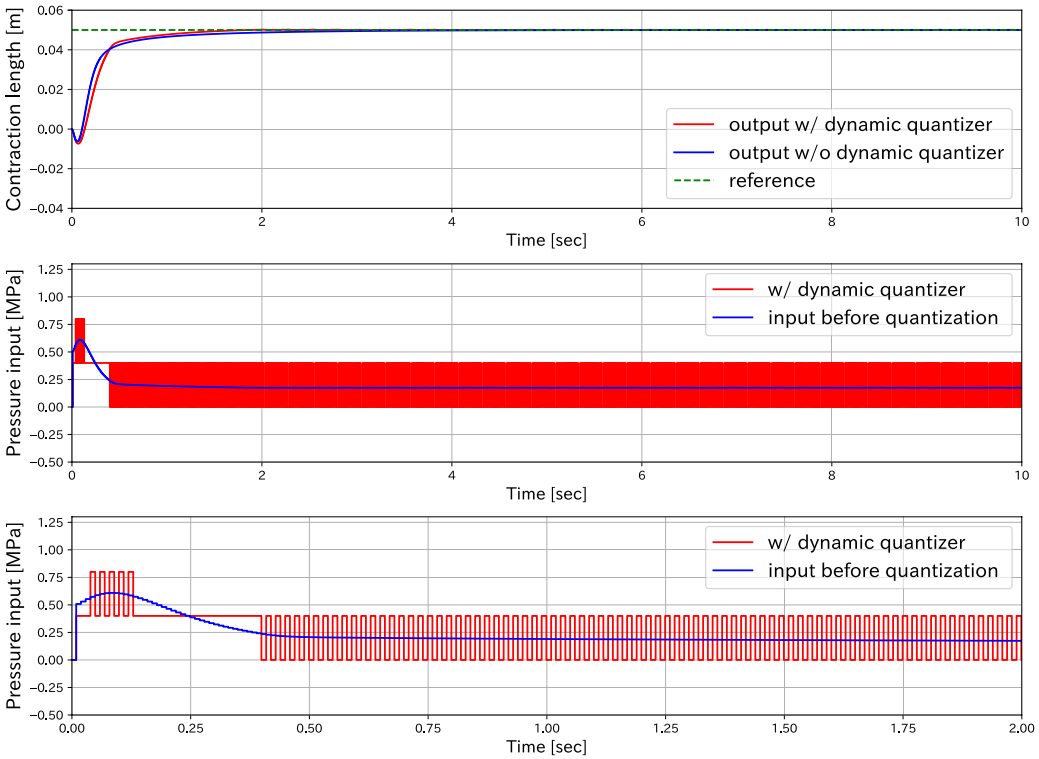

Fig. 10 Simulation result for a step reference $\bar{x}(k) = 0.05$ m

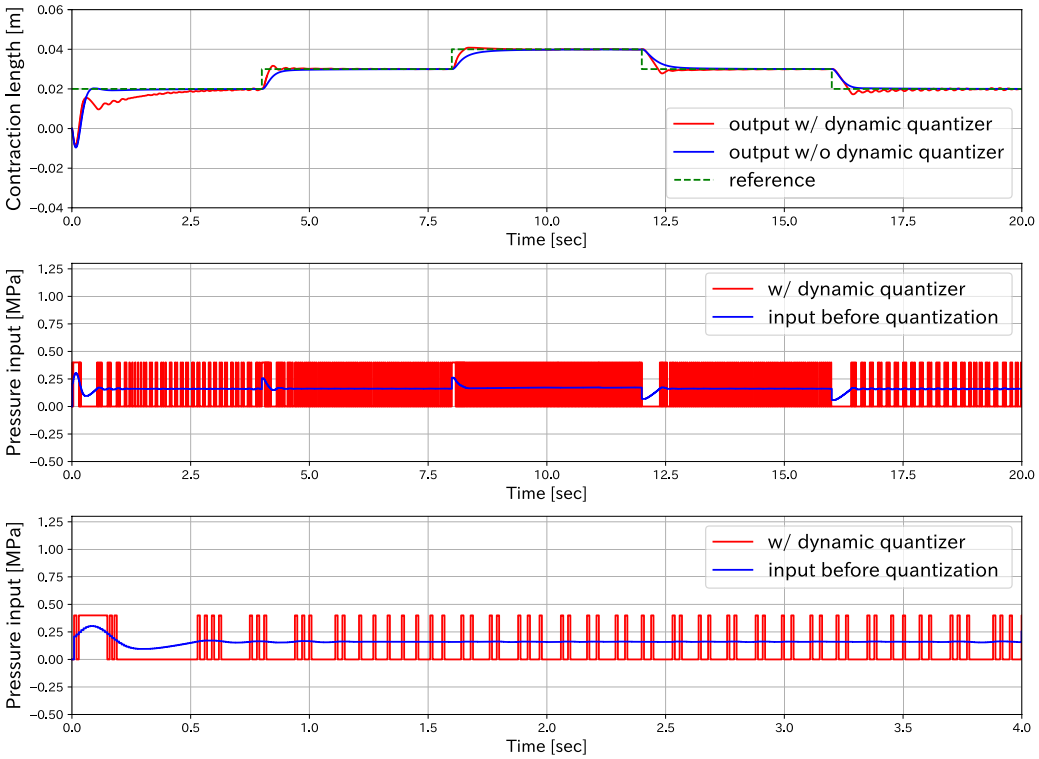

Fig. 11 Simulation result for a staircase reference

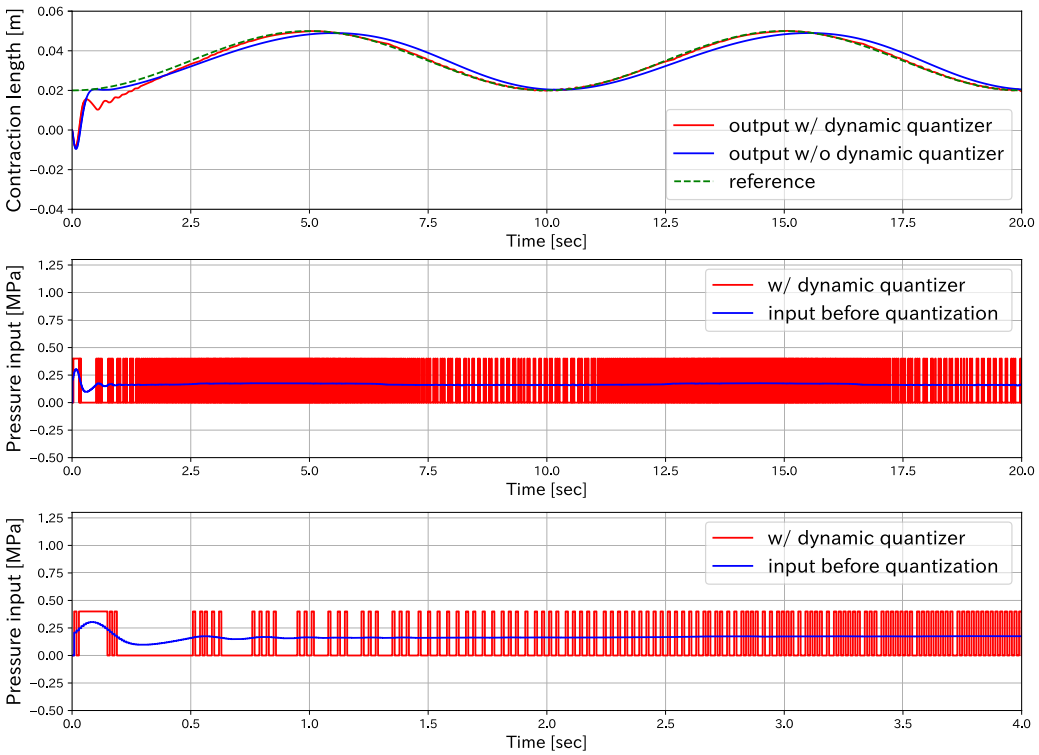

Fig. 12 Simulation result for a sinusoidal wave reference $\tilde{x}(k) = 0.02(1 - \cos(0.2\pi T_s k))$ m

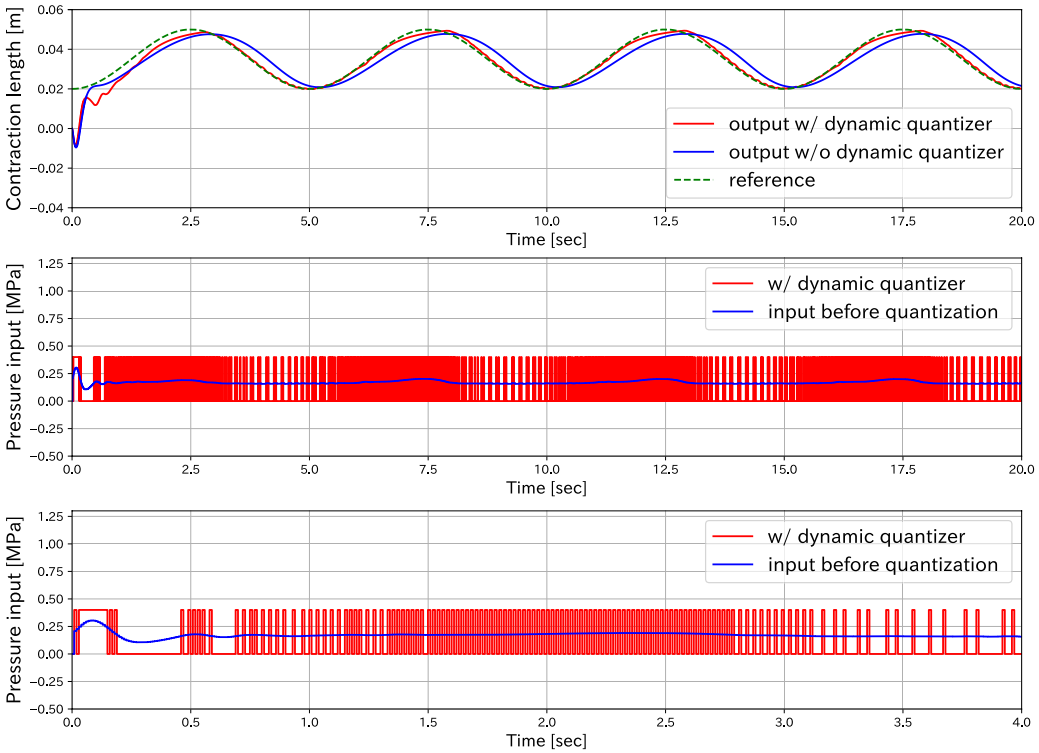

Fig. 13 Simulation result for a sinusoidal wave reference $\tilde{x}(k) = 0.02(1 - \cos(0.4\pi T_s k))$ m

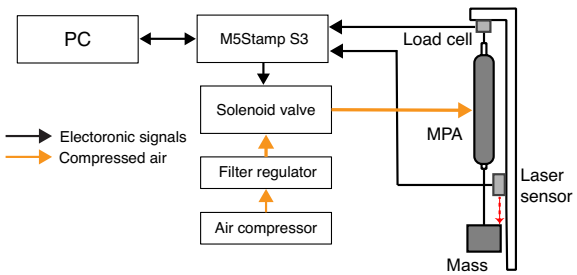

Fig. 14 Configuration of the experimental setup

Experimental setup

Overview of the experimental system configuration and setup for verifying MPA length control using the dynamic quantizer and solenoid valve are given in Figs. 14 and 15, respectively. The MPA used in the verification experiment was equivalent to that used in the previous study [23]. The unloaded length of MPA was $L_0 = 0.290$ m. A weight was connected to the MPA via a wire; the other end was connected to a load cell (Kyowa: LUX-B-1KN-ID) to measure the exerted tension of the MPA. In this experiment, the load cell was not used for control but to check for excessive loads. A microlaser distance sensor (Panasonic: HG-C1200) was used to measure the

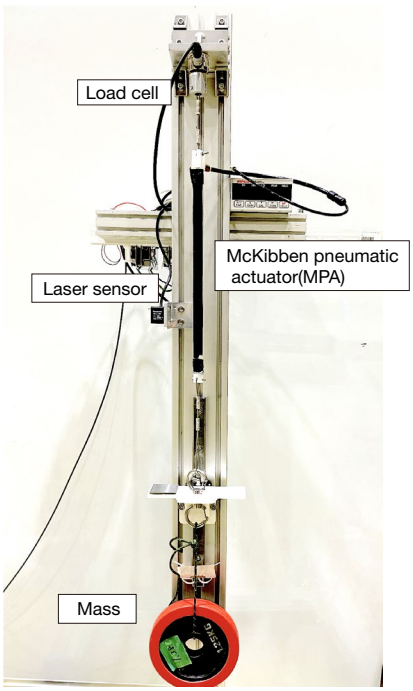

Fig. 15 Overview of experimental setup

contraction length of MPA. A M5Stamp S3 microcontroller was used to control the inputs and outputs. The sensor values were obtained with the M5Stamp S3; the controller and dynamic quantizer were implemented on the M5Stamp S3 to control the solenoid valve (SMC: S070C-SDG-32). In this study, the compressed air from the air compressor was regulated to 0.4 MPa using a filter regulator. Regulated compressed air was supplied to the MPA through a solenoid valve. Thus, 0.4 MPa of compressed air was applied to the MPA when the solenoid valve was open; otherwise, air was released, and 0 MPa air was applied. The control cycle was set to $T_s = 0.01$ s. Because the response time of the solenoid valve is 0.003 s, The opening and closing of the valve were sufficiently quick for the control cycle. Figure 16 shows the solenoid valve and microcontroller used in the experiments. Because the microcomputer and solenoid valve are small, MPA control is possible using a compact control system.

Experimental result

Similar to that in the simulations, the target contraction length used is as follows:

- Step reference $\tilde{x}(k) = 0.01, 0.02, 0.03, 0.04, 0.05$ m
- Sinusoidal reference $\tilde{x}(k) = 0.02(1 - \cos(2\pi f T_s k))$ m, where $f = 0.1, 0.2$
- Staircase reference $\tilde{x}(k) = 0.02, 0.03, 0.04$ m.

Moreover, the same values of PI controller gain and dynamic quantizer, as in the simulation, were used. For comparison, an experiment with input discretization using the PWM output function of the M5Stamp S3 (PWM frequency 100 Hz) was also conducted.

The experimental results for each reference trajectory are shown in Figs. 17, 18, 19, 20, 21, 22, 23, 24. The upper, middle, and lower parts represent the contraction x, the pressure input, and the enlarged pressure input, respectively. In the figure investigating contraction length x, the red and dotted green lines indicate results with the dynamic quantizer (red line) and reference trajectories, respectively. In the pressure input figure, the blue and red lines represent continuous input before quantization and the results without the dynamic quantizer, respectively. The enlarged graph of pressure input shows the pressure input from the beginning of the experiment to a few seconds after to clearly how the valve is switched on and off. The dynamic quantizer quantizes the input in increments of $d = 0.4$. Therefore, as in the simulation, there are cases where the quantized input has values other than 0 and 0.4 MPa. Therefore, the actual control strategy was to open and close the valve when the input value was above 0.4 MPa and below 0 MPa, respectively. The results when PWM was used are shown in Figs. 25 $\sim$ 28. For comparison, these figures also show the results of the proposed method with dynamic quantizers under the same conditions.

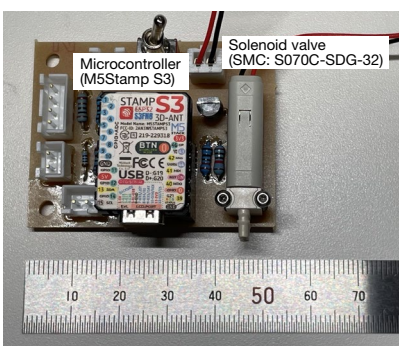

Fig. 16 The solenoid valve and the microcontroller

From Figs. 17 $\sim$ 24, it can be confirmed that the proposed control method using the dynamic quantizer can track the target value with almost no steady-state deviation, although overshoot and slight oscillations remain. In all cases, the continuous value of the pressure input under the steady state ranged from 0 to 0.4 MPa. This pressure input was difficult to achieve using solenoid valves, which use either 0 or 0.4 MPa as the input pressure. The results confirm that a dynamic quantizer can realize such pressure input and achieve tracking control. In the simulation, a negative overshoot is observed in the transient response, but no such response is observed in the experiment. This is because the actual MPA does not extend beyond its no-load length. The MPA model used in the simulation does not reflect this characteristic, causing a difference in the transient response between the simulation and experiment.

For a quantitative comparison of the control performance of the proposed method and PWM, the rising time, 10% settling time, and RMSE of the last 3 s for step references were calculated from the experimental results. The results are shown in Table 3. Compared to the results obtained using PWM, the settling time was much smaller with the proposed method when $\bar{x}(k) = 0.04$ m (Fig. 25). The rising time was slightly faster with the proposed method when $\bar{x}(k) = 0.02$ m (Fig. 26). For both $\bar{x}(k) = 0.04$ and 0.02 m, the RMSE was slightly better with the proposed method than with PWM. The average phase delay from the sinusoidal target reference for the proposed method and PWM were calculated as 0.2639 and 0.7225 rad, respectively. Therefore, the delay in following a sinusoidal reference trajectory is better with the dynamic quantizer than with PWM (Fig. 27). These results confirm that the proposed method performs as well as or better than PWM. The response using PWM may be improved by adjusting the PWM frequency.

Table 3 Comparison of control performance with dynamic quantizer and PWM for step target references

Reference (m)	Rising time (sec)		Settling time (sec)		RMSE (m)	
	Dynamic quantizer	PWM	Dynamic quantizer	PWM	Dynamic quantizer	PWM
0.02	0.3100	0.4300	2.323	2.452	2.069×10^{-3}	2.264×10^{-3}
0.04	0.8300	0.6000	0.9700	3.341	4.987×10^{-3}	5.833×10^{-3}

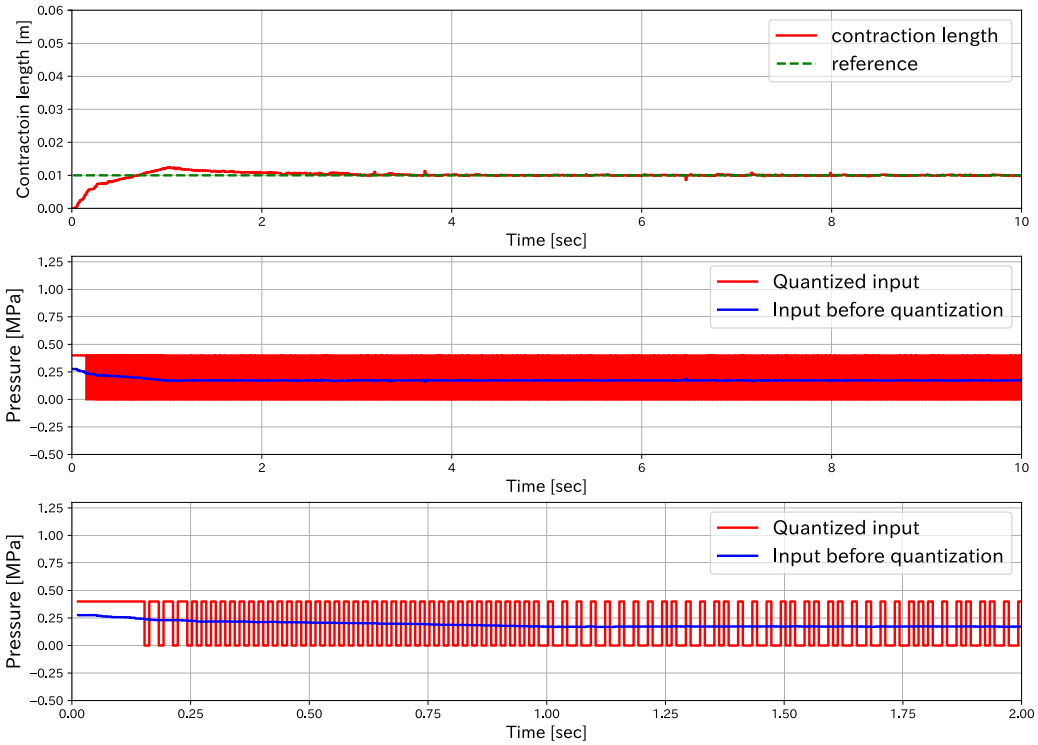

Fig. 17 Experimental result for a step reference $\bar{x}(k) = 0.01$ m

However, because the response time of the solenoid valve is 0.003 s, even if the PWM frequency is increased above the current value (100 Hz), the valve will not open and close in time. Although modified-PWM methods [14, 15] can improve system performance, these methods require multiple parameter tuning according to the valve and MPA. Therefore, it is possible, but not always easy, to improve performance with PWM. Moreover, quantization using PWM is not theoretically guaranteed, and performance degradation or instability may occur under certain circumstances. In contrast, dynamic quantizers can be designed by determining the system and controller to be controlled. It allows selecting a controller that does not destabilize, and its effect on the performance can be evaluated using $E(Q)$. Therefore, although the currently confirmed performance difference from the PWM case is slight, using a dynamic quantizer to control MPA length is considered significant enough.

These results confirm that MPA length control using dynamic quantizers is feasible in practice and demonstrate the effectiveness of the proposed method. Additionally, the compensating effect of the dynamic quantizer on the delay when tracking sinusoidal targets was confirmed through simulations. This effect may be a hidden feature of the dynamic quantizer. However, the verification of this effect is a subject for future work.

Conclusion

In our previous study [18], we proposed a method for controlling the tension of MPAs using a solenoid valve as a first step in applying dynamic quantizers to MPA control. In this study, as a second step, we proposed a method for controlling the length of a single MPA using a solenoid valve. The proposed method uses small solenoid valves that can only be opened and closed and a dynamic quantizer that converts continuous-valued inputs into

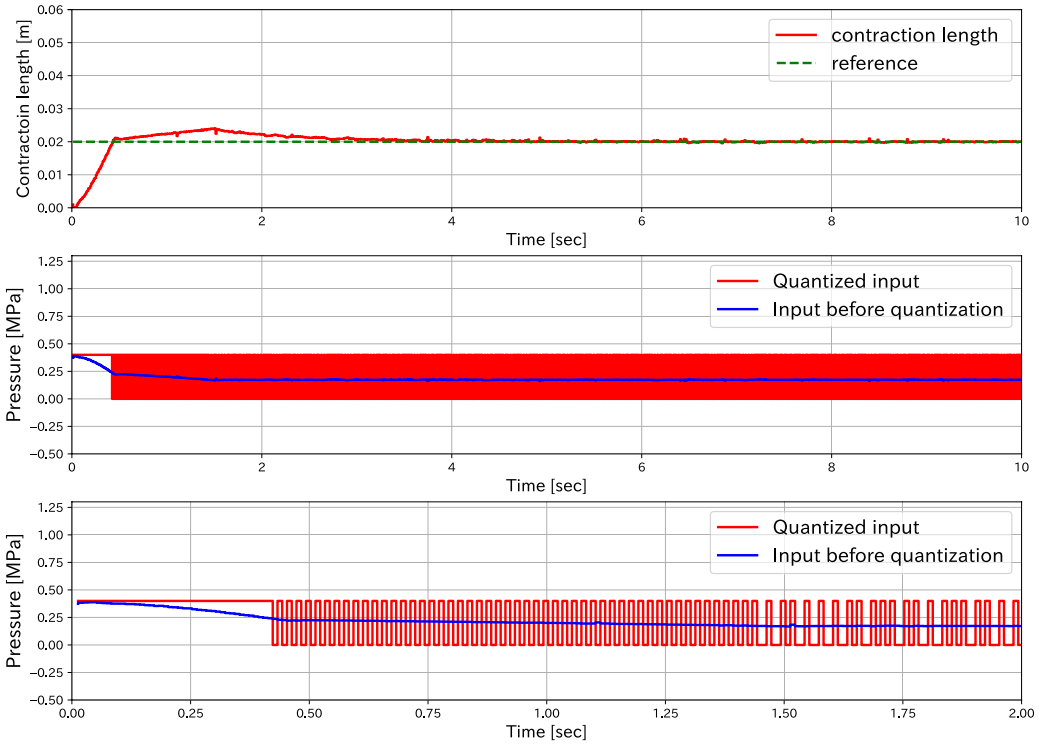

Fig. 18 Experimental result for a step reference $\bar{x}(k) = 0.02$ m

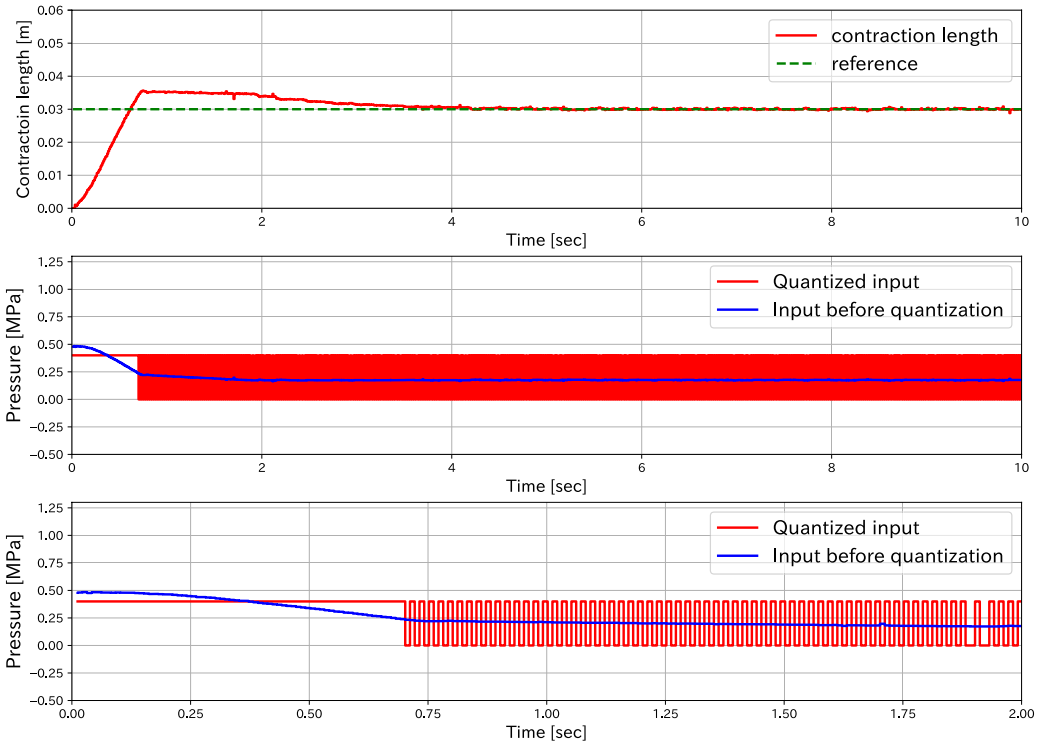

Fig. 19 Experimental result for a step reference $\bar{x}(k) = 0.03$ m

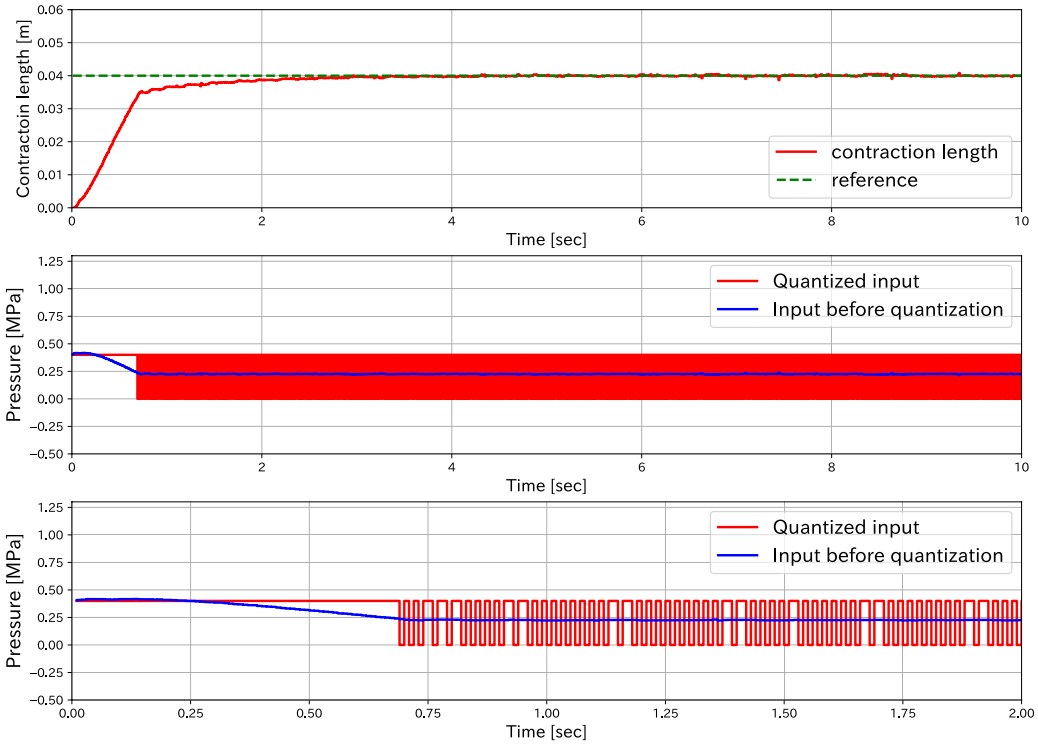

Fig. 20 Experimental result for a step reference $\bar{x}(k) = 0.04$ m

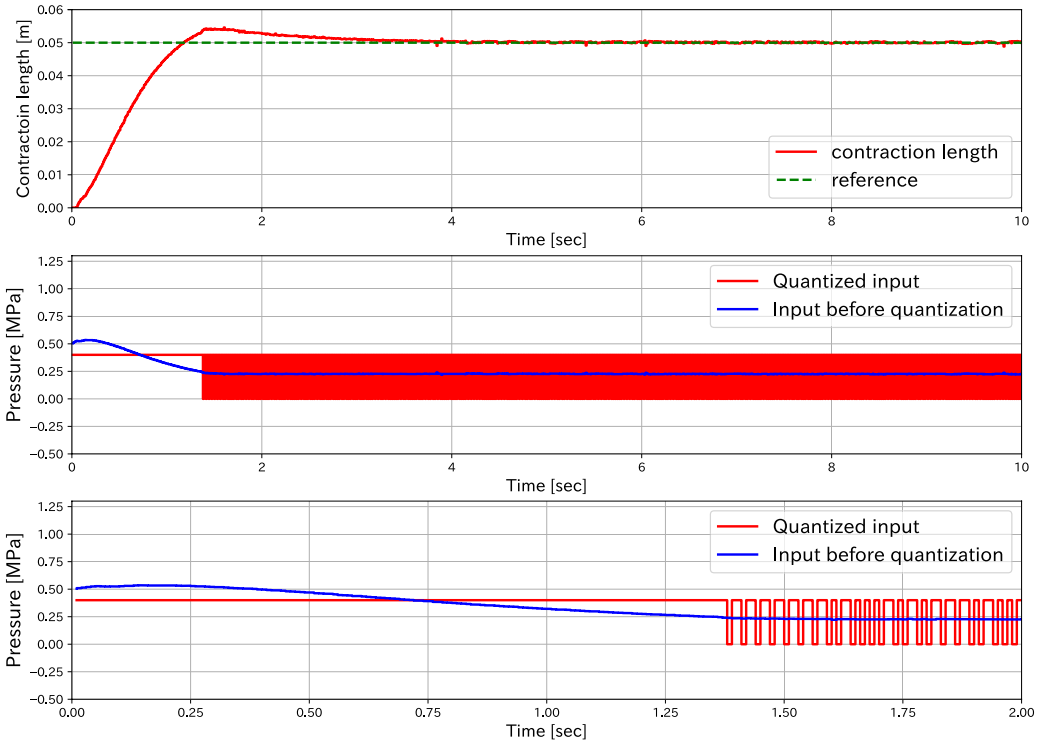

Fig. 21 Experimental result for a step reference $\bar{x}(k) = 0.05$ m

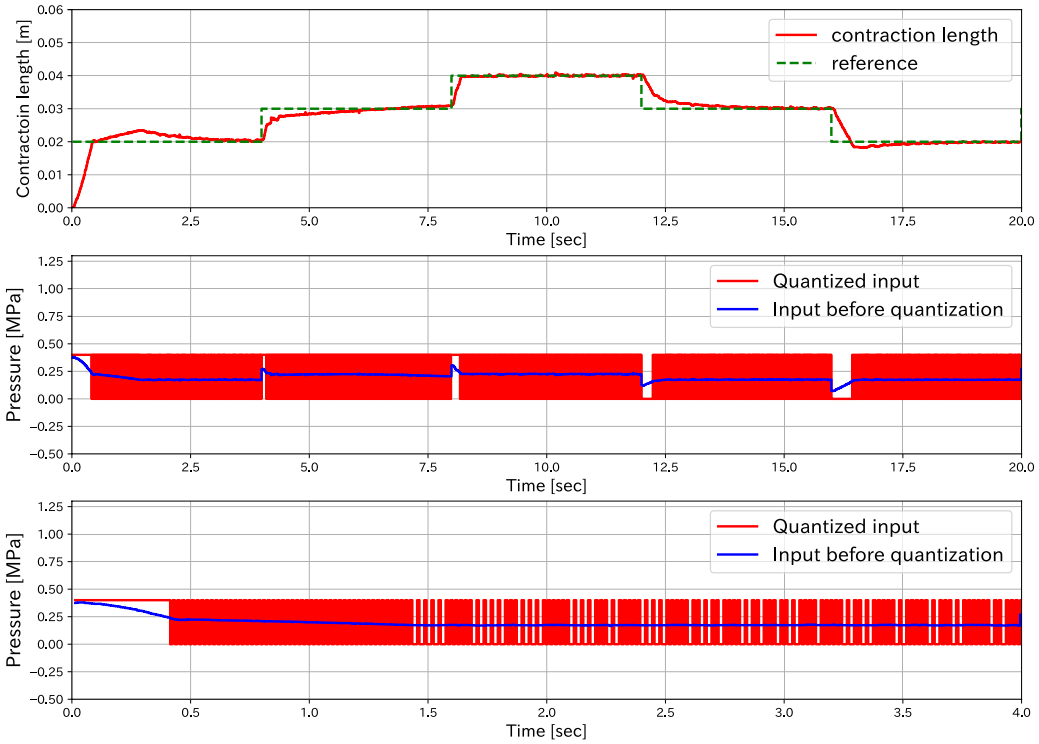

Fig. 22 Experimental result for a staircase reference

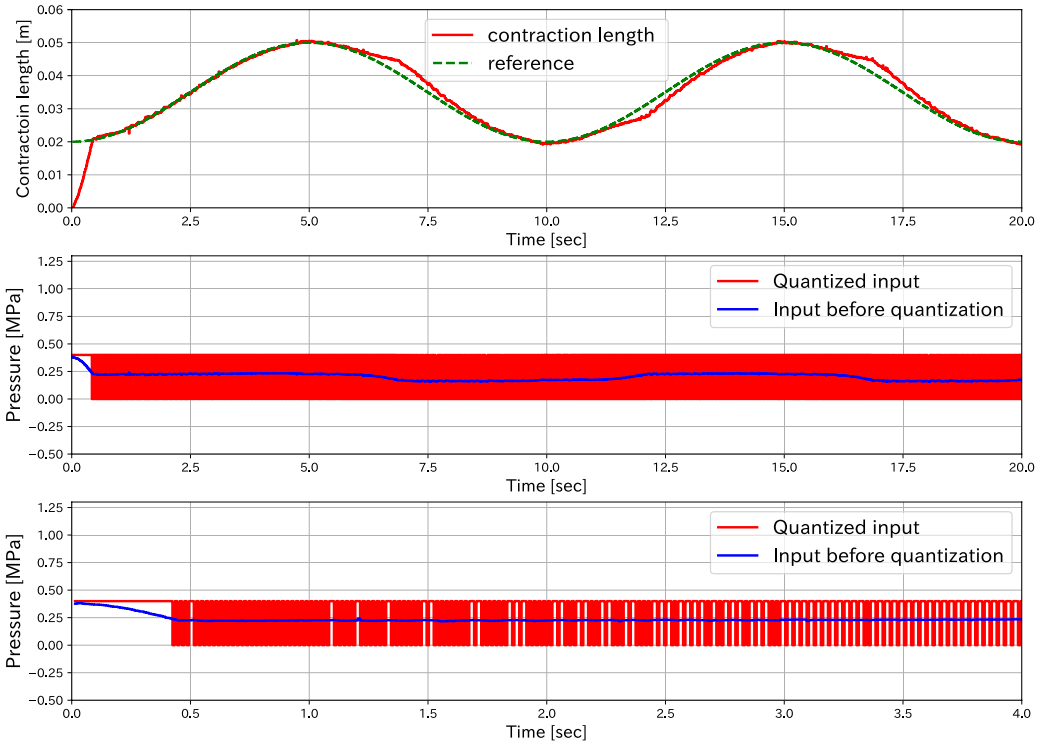

Fig. 23 Experimental result for a sinusoidal wave reference $\tilde{x}(k) = 0.02(1 - \cos(0.2\pi T_s k))$ m

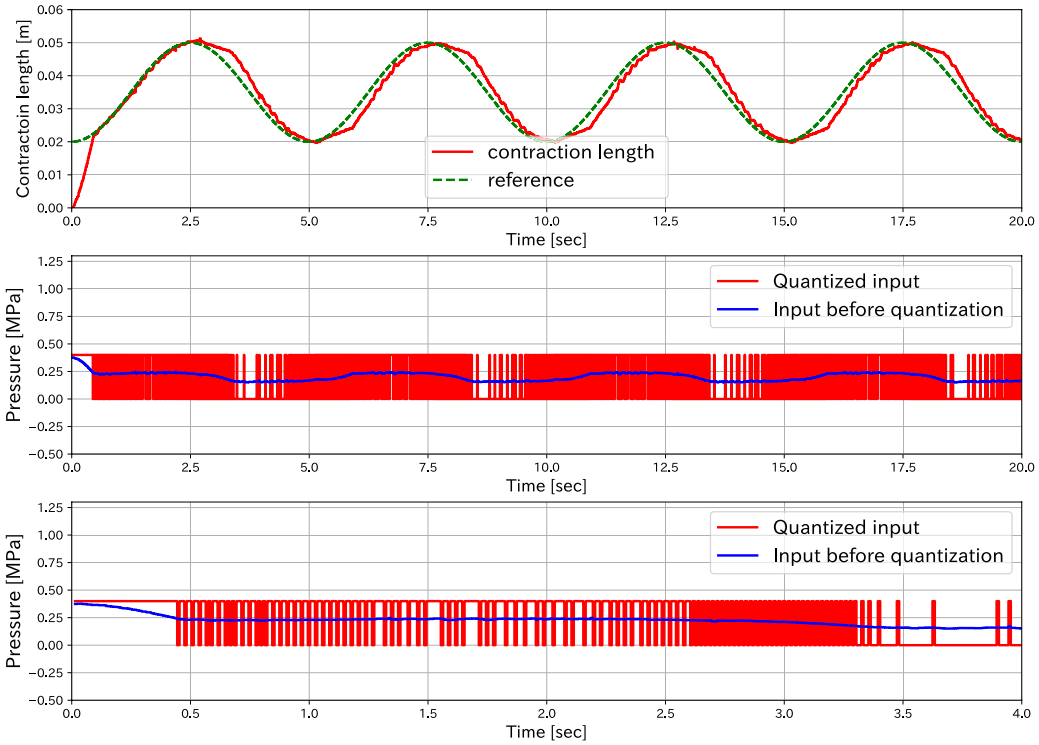

Fig. 24 Experimental result for a sinusoidal wave reference $\tilde{x}(k) = 0.02(1 - \cos(0.4\pi T_s k))$ m

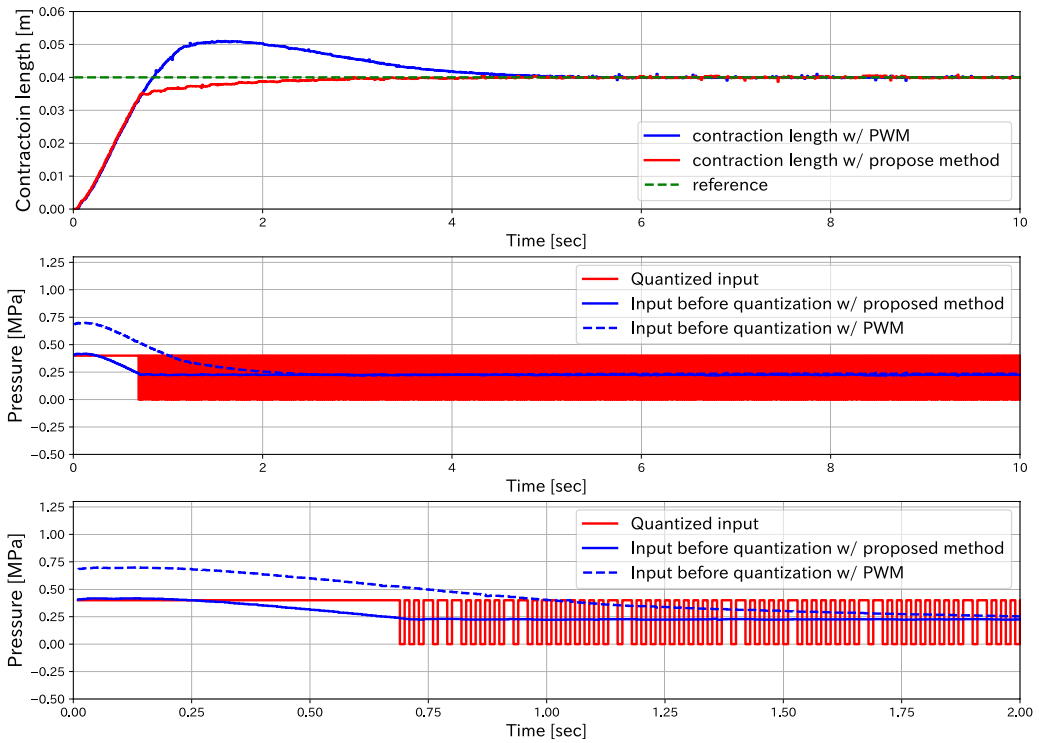

Fig. 25 Experimental result for a step reference $\bar{x}(k) = 0.04$ m with PWM

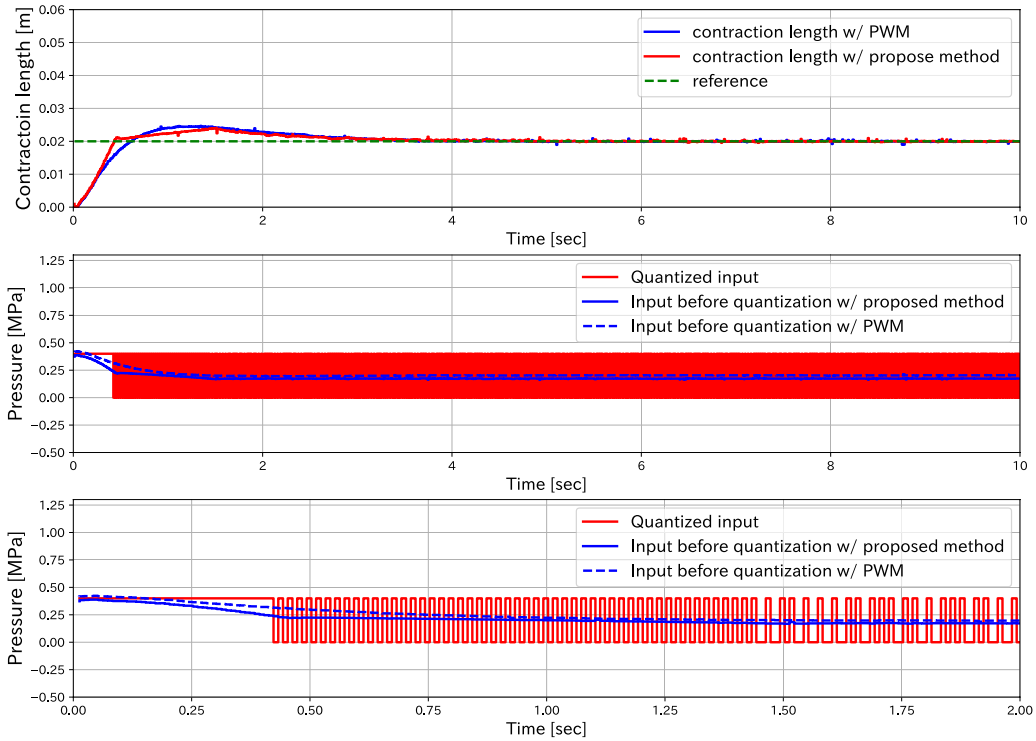

Fig. 26 Experimental result for a step reference $\bar{x}(k) = 0.02$ m with PWM

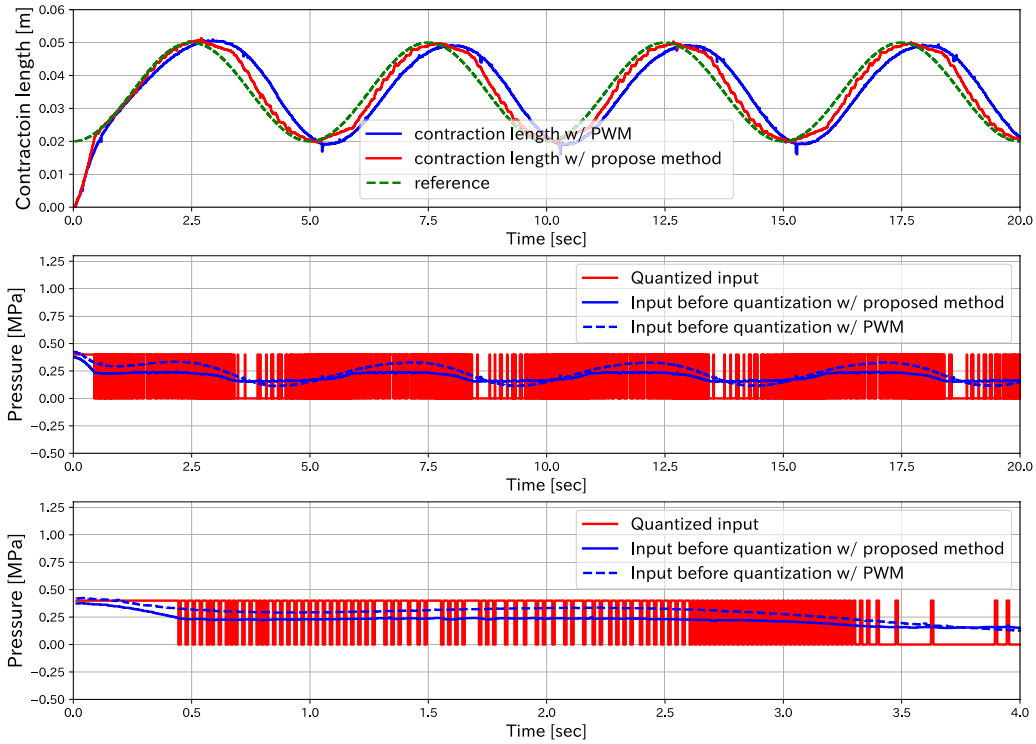

Fig. 27 Experimental result for a sinusoidal wave reference $\tilde{x}(k) = 0.02(1 - \cos(0.4\pi T_s k))$ m with PWM

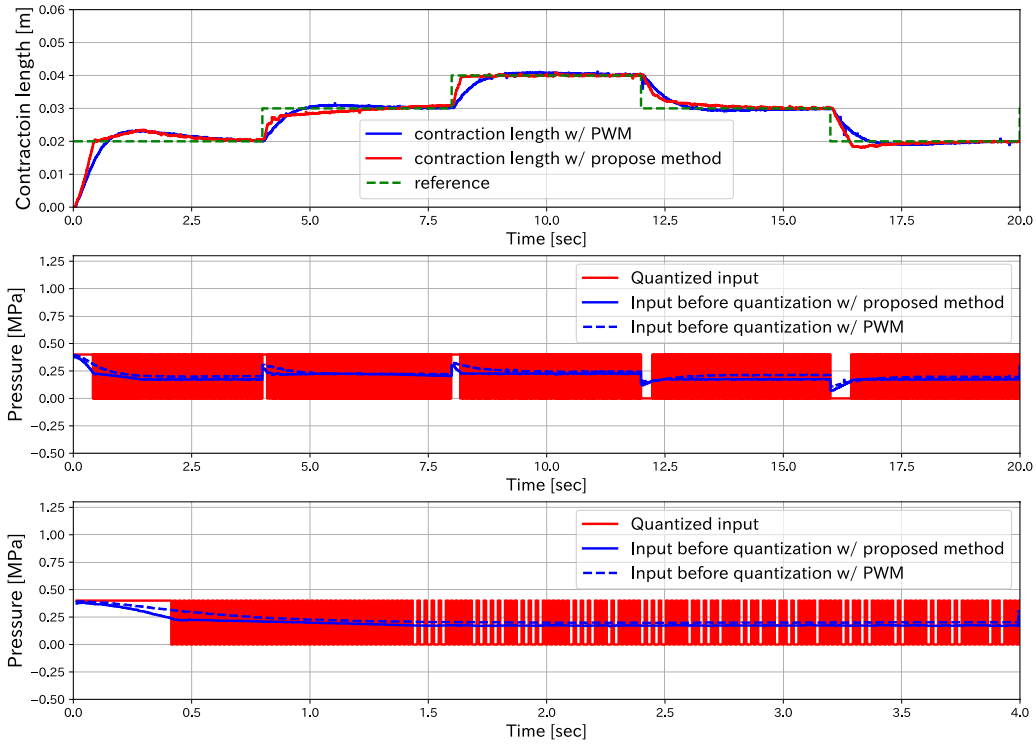

Fig. 28 Experimental result for a staircase reference with PWM

discrete inputs. The proposed method was applied to the feedback control of MPA length. Numerical simulations and experiments on actual equipment demonstrated sufficient control performance. Specifically, the proposed method exhibited a sufficiently high tracking performance using only a simple MPA model and a simple control.

The proposed method is considered sufficiently useful because sufficient control performance is confirmed. However, a quantitative evaluation of the proposed method to improve its control performance is a future task. Moreover, in actual robots, the joints are often driven by antagonizing multiple MPAs, which must be controlled in a coordinated manner. Extending the proposed method to control multiple MPAs will be a future work. Another issue to be verified is durability. The proposed method requires the valve to be switched on and off at higher speeds than typical usage of the valve. This can be a major factor in shortening the life of the valve. After the experiment in section "Experimental verification", a one-hour continuous operation test was conducted. It was confirmed that there was no significant heat generation and the control board, including the valve, was not damaged. However, verification of the durability of the proposed method, including verification of experiments over longer periods, is needed in the future.

Acknowledgements
We would like to express our sincere gratitude to Dr. Yuki Minami at Osaka University for his support in utilizing NQLib.

Author contributions
YS developed the proposed method and conducted the simulation analysis and experiments. KN and DN supported developing the experimental setup and discussing the simulation and experiment results. KO used his extensive knowledge of control theory to support this research. All authors have read and approved the manuscript.

Funding
This study was supported by JSPS KAKENHI (grant numbers JP21H01276, JP22K19795, JP23H01435 and JP23K13280).

Availability of data, materials and code
The data supporting the findings of this study are available from the corresponding author, YS, upon reasonable request.

Declarations

Ethics approval and consent to participate
Not applicable.

Consent for publication
Not applicable.

Competing interests
The authors declare no competing interests.

Received: 31 December 2023 Accepted: 21 April 2024
Published online: 02 May 2024

References

1. Agerholm M, Lord A (1961) The artificial muscle of Mckibben. Lancet 277(7178):660–661. https://doi.org/10.1016/S0140-6736(61)91676-2
2. Gavrilović MM, Marić MR (1969) Positional servo-mechanism activated by artificial muscles. Med Biol Eng 7(1):77–82. https://doi.org/10.1007/BF02474672
3. Faudzi AAM, Endo G, Kurumaya S, Suzumori K (2018) Long-legged hexapod giacometti robot using thin soft Mckibben actuator. IEEE Robot Autom Lett 3(1):100–107. https://doi.org/10.1109/LRA.2017.2734244
4. Niiyama R, Nagakubo A, Kuniyoshi Y (2007) Mowgli: a bipedal jumping and landing robot with an artificial musculoskeletal system. In: Niiyama R (ed) Proceedings 2007 IEEE international conference on robotics and automation. IEEE, Rome, pp 2546–2551. https://doi.org/10.1109/ROBOT.2007.363848
5. Takuma T, Hosoda K (2006) Controlling the walking period of a pneumatic muscle walker. Int J Robot Res 25(9):861–866. https://doi.org/10.1177/0278364906069187
6. Tondu B, Ippolito S, Daidie A, Tondu B, Ippolito S, Seven-degrees-of-freedom ADA (2005) A seven-degrees-of-freedom robot-arm driven by pneumatic artificial muscles for humanoid robots. Int J Robot Res 24(4):257–274. https://doi.org/10.1177/0278364905052437
7. Wisse M, Von Frankenhyyzen J (2003) Design and construction of MIKE; a 2-D autonomous biped based on passive dynamic walking. In: Kimura H, Tsuchiya K, Ishiguro A, Witte H (eds) Adapt motion Anim Mach. Springer, Tokyo, pp 143–154. https://doi.org/10.1007/4-431-31381-8_13
8. Andrikopoulos G, Nikolakopoulos G, Manesis S (2013) Pneumatic artificial muscles: a switching model predictive control approach. Control Eng Pract 21(12):1653–1664. https://doi.org/10.1016/j.conengprac.2013.09.003
9. Andrikopoulos G, Nikolakopoulos G, Manesis S (2014) Advanced nonlinear PID-based antagonistic control for pneumatic muscle actuators. IEEE Trans Ind Electron 61(12):6926–6937. https://doi.org/10.1109/TIE.2014.2316255
10. Cao Y, Huang J (2020) Neural-network-based nonlinear model predictive tracking control of a pneumatic muscle actuator-driven exoskeleton. IEEE/CAA J Autom Sin 7(6):1478–1488. https://doi.org/10.1109/JAS.2020.1003351
11. Robinson RM, Kothera CS, Sanner RM, Wereley NM (2016) Nonlinear control of robotic manipulators driven by pneumatic artificial muscles. IEEE/ASME Trans Mech 21(1):55–68. https://doi.org/10.1109/TMECH.2015.2483520
12. Shin T, Ibayashi T, Kogiso K (2022) Detailed dynamic model of antagonistic PAM system and its experimental validation: sensorless angle and torque control with UKF. IEEE/ASME Trans Mech 27(3):1715–1726. https://doi.org/10.1109/TMECH.2021.3086218. arxiv:2009.09229
13. Jouppila VT, Gadsden SA, Bone GM, Ellman AU, Habibi SR (2014) Sliding mode control of a pneumatic muscle actuator system with a PWM strategy. Int J Fluid Power 15(1):19–31. https://doi.org/10.1080/14399776.2014.893707
14. Ham RV, Verrelst B, Daerden F, Lefeber D (2003) Pressure control with on-off valves of pleated pneumatic artificial muscles in a modular one-dimensional rotational joint. In: International conference on humanoid robots
15. Jien S, Hirai S, Ogawa Y, Ito M, Honda K (2009) Pressure control valve for McKibben artificial muscle actuators with miniaturized unconstrained pneumatic on/off valves. In: 2009 IEEE/ASME International conference on advanced intelligent mechatronics. Singapore, IEEE, pp 1383–1388. https://doi.org/10.1109/AIM.2009.5229882
16. Azuma S-I, Sugie T (2008) Optimal dynamic quantizers for discrete-valued input control. Automatica 44(2):396–406. https://doi.org/10.1016/j.automatica.2007.06.012
17. Minami Y, Azuma S-I, Sugie T (2007) An optimal dynamic quantizer for feedback control with discrete-valued signal constraints. In: 2007 46th IEEE Conference on Decision and Control. IEEE, New Orleans, pp 2259–2264. https://doi.org/10.1109/CDC.2007.4434167
18. Sugimoto Y, Naniwa K, Nakanishi D, Osuka K (2023) Tension control of a Mckibben pneumatic actuator using a dynamic quantizer. J Robot Mech 35(4):1038–1046. https://doi.org/10.20965/jrm.2023.p1038
19. Klute GK, Czerniecki JM, Hannaford B (2002) Artificial muscles: actuators for biorobotic systems. Int J Robot Res 21(4):295–309. https://doi.org/10.1177/027836402320556331
20. Tondu B, Lopez P (2000) Modeling and control of McKibben artificial muscle robot actuators. IEEE Control Syst Mag 20(2):15–38. https://doi.org/10.1109/37.833638
21. Chou C-P, Hannaford B (1996) Measurement and modeling of McKibben pneumatic artificial muscles. IEEE Trans Robot Autom 12(1):90–102. https://doi.org/10.1109/70.481753
22. Sugimoto Y, Naniwa K, Osuka K, Sankai Y (2013) Static and dynamic properties of McKibben pneumatic actuator for self-stability of legged-robot motion. Adv Robot. https://doi.org/10.1080/01691864.2013.763007
23. Nakanishi D, Sugimoto Y, Honda H, Osuka K (2016) Experiments and analysis for modeling of Mckibben pneumatic actuator. J Robot Mech 28(6):830–836. https://doi.org/10.20965/jrm.2016.p0830
24. Goto T, Sugimoto Y, Nakanishi D, Naniwa K, Osuka K (2021) Analysis of autonomous coordination between actuators in the antagonist musculoskeletal model. J Robot Mech 33(2):410–420. https://doi.org/10.20965/jrm.2021.p0410
25. Azuma S-I, Minami Y, Sugie T (2011) Optimal dynamic quantizers for feedback control with discrete-level actuators: unified solution and experimental evaluation. J Dyn Syst Meas Control Trans ASME 133(2):1–10. https://doi.org/10.1115/1.4002952
26. Azuma S-I, Sugie T (2008) Synthesis of optimal dynamic quantizers for discrete-valued input control. IEEE Trans Autom Control 53(9):2064–2075. https://doi.org/10.1109/TAC.2008.929400
27. Sawada K, Shin S (2011) Synthesis of decentralized dynamic quantizer within invariant set analysis framework. IFAC Proc Vol (IFAC-PapersOnline) 44(1 PART 1):11284–11289. https://doi.org/10.3182/20110828-6-IT-1002.01963
28. Azuma S-I, Morita R, Minam Y, Sugie T (2008) A software tool for control-oriented dynamic quantizer design and experimental evaluation. Trans Instit Syst Control Inform Eng 21(12):408–416. https://doi.org/10.5687/iscie.21.408
29. Morita R, Azuma S-I, Minami Y, Sugie T (2011) Graphical design software for dynamic quantizers in control systems. SICE J Control Meas Syst Integr 4(5):372–379. https://doi.org/10.9746/jcmsi.4.372
30. NQLib Website. https://pypi.org/project/nqlib/. Accessed 25 Apr 2024
31. Ishikawa M, Maruta I, Sugie T (2008) Compensation of actuator nonlinearity using discrete-valued input control based on feedback modulator. Trans Soc Instrum Control Eng 44(3):288–290. https://doi.org/10.9746/ve.sicetr1965.44.288
32. Ohgi T, Yokokohji Y (2008) Control of hydraulic actuator systems using feedback modulator. J Robot Mech 20(5):695–708. https://doi.org/10.20965/jrm.2008.p0695

Publisher's Note